Swept-3-D Ultrasound Imaging of the Mouse Brain Using a Continuously Moving 1-D-Array—Part II: Functional Imaging
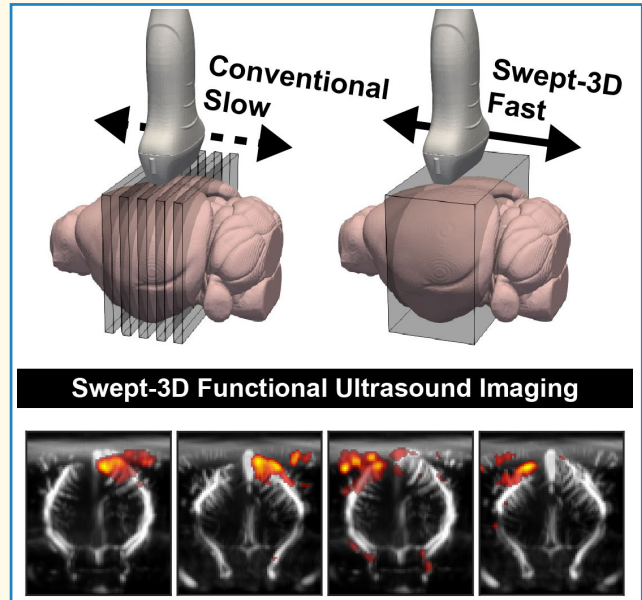
Bastian S. Generowicz, Stephanie Dijkhuizen, Laurens W. J. Bosman, Chris I. De Zeeuw, Sebastiaan K. E. Koekkoek, and Pieter Kruizinga

Abstract—**Functional ultrasound (fUS) using a 1-D-array transducer normally is insufficient to capture volumetric functional activity due to being restricted to imaging a single brain slice at a time. Typically, for volumetric fUS, functional recordings are repeated many times as the transducer is moved to a new location after each recording, resulting in a nonunique average mapping of the brain response and long scan times. Our objective was to perform volumetric 3-D fUS in an efficient and cost-effective manner. This was achieved by mounting a 1-D-array transducer to a high-precision motorized linear stage and continuously translating over the mouse brain in a sweeping manner. We show how the speed at which the 1-D-array is translated over the brain affects the sampling of the hemodynamic response (HR) during visual stimulation as well as the quality of the resulting power Doppler image (PDI). Functional activation maps were compared between stationary recordings, where only one functional slice is obtained for every recording, and our swept-3-D method, where volumetric fUS was achieved in a single functional recording. The results show that the activation maps obtained with our method closely resemble those obtained during a stationary recording for that same location, while our method is not restricted to functional imaging of a single slice. Lastly, a mouse brain subvolume of ~6 mm is scanned at a volume rate of 1.5 s per volume, with a functional PDI reconstructed every 200 μm, highlighting swept-3-D's potential for volumetric fUS. Our method provides an affordable alternative to volumetric fUS using 2-D-matrix transducers, with a high SNR due to using a fully sampled 1-D-array transducer, and without the need to repeat functional measurements for every 2-D slice, as is most often the case when using a 1-D-array. This places our swept-3-D method as a potentially valuable addition to conventional 2-D fUS, especially when investigating whole-brain functional connectivity, or when shorter recording durations are desired.**

Index Terms—**3-D mouse brain, functional ultrasound (fUS), motorized linear stage, ultrafast Doppler, whole-brain Doppler imaging.**

Swept-3D Functional Ultrasound Imaging

I. Introduction

FUNCTIONAL ultrasound (fUS) may present itself as a valuable technique to be used in the field of neuroscience, that is among other things, due to its high spatial and temporal resolutions when compared to methods such as functional magnetic resonance imaging (fMRI). fUS makes use of high frame-rate power Doppler images (PDIs) to measure blood hemodynamics, which can be interpreted as a proxy for neuronal activity due to the mechanism of neurovascular coupling [1].

Typically, fUS of the mouse brain relies on a 1-D-array ultrasound transducer to gather data from a single 2-D slice over time, while a stimulation paradigm is presented to the subject. The obtained Doppler signal for every image pixel is then correlated with the input stimulus [often convolved with

Highlights

- **Swept-3-D functional ultrasound (fUS) imaging allows for volumetric functional imaging of a mouse brain by continuously sweeping a 1-D-array transducer over the craniotomy.**

- **Swept-3-D fUS can image the visual pathways in a 6 mm^3 subvolume of a mouse brain at 1.5 s per volume with similar functional sensitivity as that of stationary 2-D recordings.**

- **Swept-3-D fUS is easy to implement and provides an affordable approach to volumetric fUS.**

a hemodynamic response function (HRF)] to create functional activation maps. This 2-D imaging method is insufficient to accurately measure a 3-D brain volume as information from functional regions outside the field of view of the 2-D slice is not included. Therefore, a unique time-bound brain response or activity manifested through the hemodynamic response (HR) that involves multiple distinct functional regions can by definition not be captured accurately in its four dimensions (3-space + 1 time). This lack of access to multiple functional regions can sometimes be remedied by placing the 1-D-array transducer in an orientation such that multiple regions of interest are present in the current field of view, such as was shown by Grohs-Metz et al. [2] while functionally imaging the prefrontal cortex and amygdala using fUS by using a navigational system with atlas registration [3], but is still restricted to a single slice per recording. In conclusion, the functional brain needs to be sampled in 3-D.

To achieve 3-D functional maps using a 1-D array, experiments are often repeated for every 2-D slice using a motorized stage [4], [5], [6]. This method of 3-D fUS inherently requires long recording times, which requires repeatability of the subject's response to the applied stimulus, and does not take into account the ability of the subject to become habituated, conditioned, and/or fatigued during repeated recordings. Bertolo et al. [7] showed that by taking very short, stationary recordings and quickly moving the 1-D-array ultrasound transducer to the next location, it was possible to perform volumetric 3-D fUS without needing repeated functional experiments, however due to the start-and-stop line-by-line scanning they were restricted to either few scanned locations, or a lower volume sample rate.

Another method for 3-D sampling of the brain is using 2-D-matrix arrays, which have been successfully applied for 3-D fUS. These matrix transducers can insonify a large volume without moving [8], [9]. While the limited field-of-view problem can be easily solved using these matrix transducers, they suffer from low sensitivity and are expensive in both computational complexity as well as monetary cost. Alternative volumetric sampling techniques such as those offered by row-column arrays have also been successfully implemented for fUS [10].

In this article, we set out to achieve 3-D fUS imaging of the brain cost-effectively by continuously translating a 1-D-array transducer back and forth over the brain. Part I of this article is focused on obtaining the best vascular images in a time-efficient manner. We show that there is a tradeoff between PDI quality and translation speed, where higher translation speeds cause less spatial coherence between successive frames, decreasing the ability to properly filter out the tissue signal and also resulting in lower SNR PDIs due to less desirable averaging effects.

The objective of this article is different from the previous one in that it tries to accurately sample a functional HR to a given stimulus while continuously translating over the brain. Nunez-Elizalde et al. [11] showed, by performing simultaneous electrode spike recordings and fUS recordings in awake mice, that the fUS blood flow signal has a direct relationship to the slow fluctuations (<0.3 Hz) in a local firing rate through an HRF, which is said to be in the order of multiple seconds. Therefore, for 3-D imaging with a swept 1-D-array transducer, from now on referred to as *swept-3-D* in this article, we need to sample every region of the brain at a high enough sampling rate to reliably be able to measure the fluctuations in blood flow signal as well as be able to robustly remove the tissue components of the ultrasound signal. In this article, we will focus on achieving the highest functional sensitivity while scanning the brain in swept-3-D.

II. Swept-3-D Ultrasound Acquisition

Swept-3-D fUS poses a couple of problems that are unique when compared to performing structural scans of blood vasculature as was shown in Part I of this article. First, for structural scans of the brain, it is only necessary to move the ultrasound transducer from the beginning of the craniotomy to the end of the craniotomy one time, referred to as a sweep. For functional imaging, as we are interested in the fluctuations of the blood signal in a brain region over time, it is necessary to be able to accurately combine Doppler frames over many sweeps. Second, while moving back and forth over the brain, the temporal sampling at each location is different depending on the location of the acquisition in the sweep. Third, most often, fUS is ideally performed on awake subjects as anesthesia has been shown to affect neurovascular coupling [12], and it allows for testing of a larger variety of functional paradigms.

A. Spatial Sampling

In conventional 2-D fUS, where the 1-D array is kept at the same location during a functional recording, a power Doppler (PD) signal is continuously acquired for every imaging pixel in the 2-D slice throughout the whole recording. As we are continuously translating back-and-forth over the brain with our method, we only obtain a PD signal for a particular 2-D slice every time the transducer passes that location, which
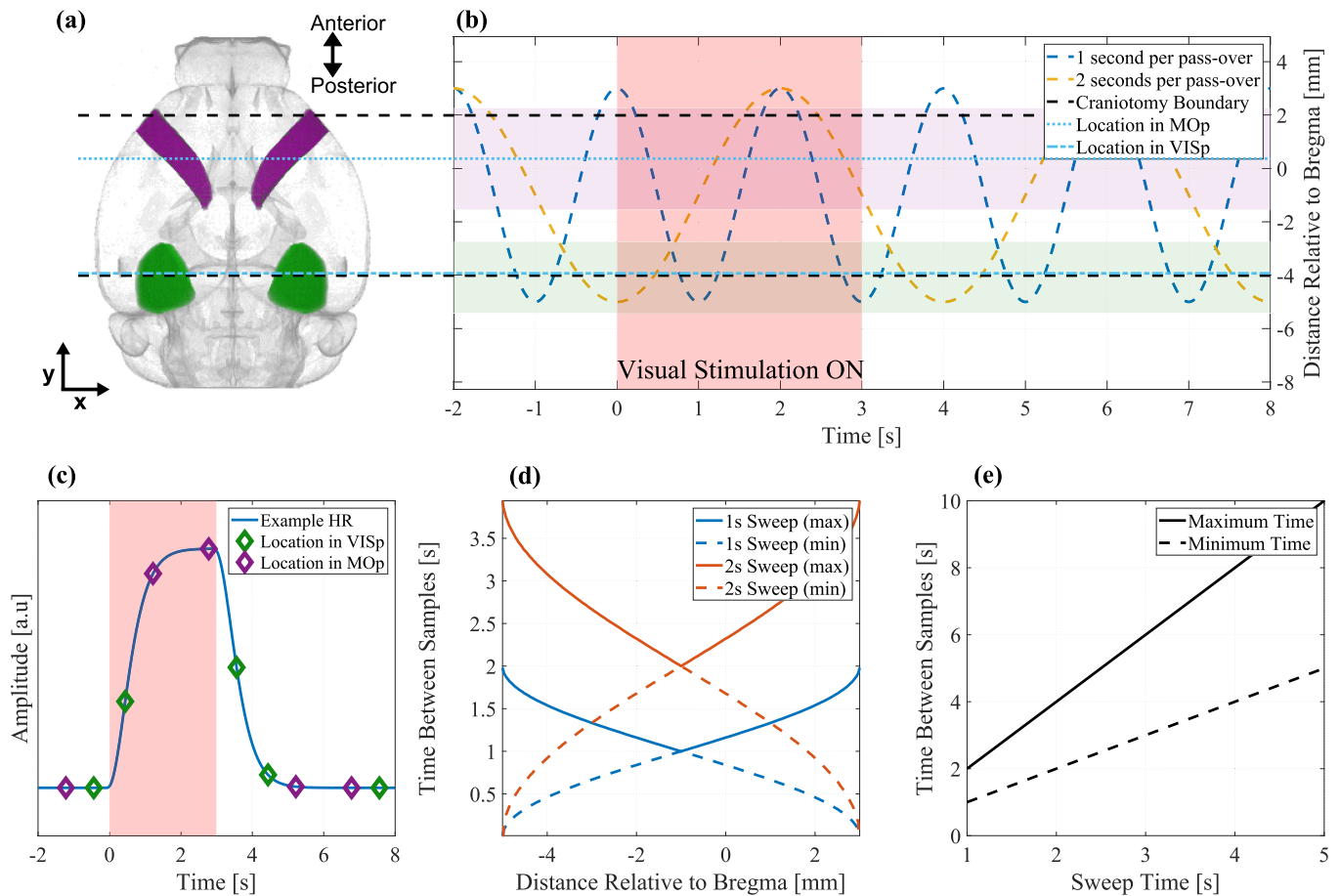
Fig. 1. Overview of ultrasound swept-3-D spatial sampling. (a) Schematic of the top view of a mouse brain with the primary visual area—VISp, and primary motor area—MOp highlighted in green and purple respectively. (b) Example simulated trajectories of the ultrasound transducer when moving from the most rostral part of the craniotomy boundary to the most caudal part (one sweep) for translation speeds of 1 and 2 s per sweep shown by the blue and orange dotted lines, respectively, while an example visual stimulation is applied for 3 s (red background). (c) For the translation speed of 2 s per sweep, the simulated sampling of an example HR (blue line) is shown for the locations in the VISp and the MOp shown in (a) and (b). Each sample obtained at the chosen locations is visualized by green and purple diamonds, respectively. (d) For specific locations along the trajectory, the minimum and maximum time between successive samples of the two translation speeds. Showing uniform sampling at the middle of the trajectory and the least uniform sampling at the edges. (e) For varying sweeping speeds, the minimum and maximum time between successive samples. For a sweep time of 2 s, there are 2 s between samples obtained at the middle of the trajectory and 4 s between samples obtained at the edges of the trajectory.

results in nonuniform sampling for every location. With fUS, we are interested in accurately sampling the transient brain hemodynamics during a functional recording, and therefore it is important to investigate how our method affects the sampled functional response.

An illustration of the unique sampling dilemma for swept-3-D fUS is shown in Fig. 1 for two example translation speeds. Here, the 1-D-array transducer is continuously moving over the brain from the most rostral boundary of the craniotomy at Bregma +2 mm to the most caudal boundary at Bregma −4 mm while a visual stimulation paradigm is presented to the subject. We opted for a sinusoidal trajectory to keep the movement smooth and prevent undesirable effects such as over- or under-shooting the set location limits, which allowed us to reliably increase the translation speed and therefore temporal sampling of every location. For every sweep of the 1-D-array transducer, a 3-D PD volume can be constructed. The period of the sinusoid determines how many volumes can be recorded per second, which is especially

important for fUS as enough volumes have to be recorded to accurately sample the hemodynamic changes during every stimulation ON/OFF-period. Fig. 1(a) shows a mouse brain with primary visual area—VISp, and primary motor area—MOp highlighted in green and purple, respectively, created using data from the Scalable Brain Atlas [13], [14]. These specific regions are shown to highlight the difference in sampling each location when continuously translating over the brain. Fig. 1(b) shows two example translation speeds over the mouse brain, for 1 s per sweep (blue dotted line), and 2 s per sweep (orange dotted line), while a 3-s visual stimulation is presented to the subject (red background). The limits of the sweep are set just past the boundaries of the craniotomy (black dotted lines) to ensure that regions close to the boundaries are sampled. For Fig. 1(c), an example HR was simulated by using a gamma-distribution function as shown by Aydin et al. [15] and Erol et al. [16], and convolving it with the example 3-s visual stimulation paradigm. Here, we can see, for a translation speed of 2 s per sweep from Fig. 1(b), that how the locations

highlighted by the dotted light blue lines in the VISp and MOp are sampled. Here, we can see that it is possible that only one sample is obtained during the stimulation ON period, which may not allow for sufficient functional sensitivity. For swept-3-D acquisitions, as we move closer toward the center of the sweep the temporal sampling becomes more uniform, meaning at the center of the sweep for a trajectory of 1 s per sweep it is sampled at 1 Hz while at the worst-case boundary of the trajectory, one sample is obtained every ∼2 s. This relationship is shown in Fig. 1(d) and (e), where Fig. 1(d) shows the minimum and maximum time between samples for 1 and 2 s per sweep, and Fig. 1(e) shows the worst (at the trajectory limits) and best (at the center of the trajectory) times between samples for varying sweep times.

Additionally, locations along a sweep will naturally be sampled at different phases of the stimulation paradigm. For the 2 s per sweep case, while the most caudal part of VISp samples the blood signal at the onset of the visual stimulation, the most rostral part of VISp samples the blood signal almost a second later. This means that if the response to the onset of a stimulus is short or fluctuates over time, later samples of VISp might be recording a different response compared to earlier ones. For functional analysis, we have to have a sufficient sweep speed to be able to accurately sample the ratio between the blood signal for the ON and OFF periods of the presented paradigm. This problem is not unique to our swept-3-D fUS method, as fMRI also uses quick switching of imaging planes during functional recordings to create full 3-D functional sensitivity maps. In fMRI, the switching of imaging planes occurs by a change in the magnetic field; therefore, the temporal resolution is directly related to the number of slices imaged [17], which means that a functional volume is typically only acquired once every few seconds [18]. Similar to fMRI, our volume rate depends on the subvolume selected for imaging (e.g., size of the craniotomy) and therefore needs to be considered to maintain a high enough temporal sampling frequency for functional analysis.

B. Repeatability of Doppler Frames

For conventional stationary fUS recordings, ultrasound data from a number of angled plane-wave transmissions is recorded, beamformed, and compounded into a single beamformed frame. The time between angled plane-wave transmissions, referred to as the pulse repetition frequency (PRF), is commonly set to a fixed value that is significantly lower than the theoretical maximum set by the time taken for the wave to propagate from the array to the end of the brain (most ventral) and back [19]. If a fixed PRF would be used during swept-3-D acquisitions, the location of each obtained ultrasound frame within a sweep would be based on the speed of the motorized stage, meaning that the sampling would be nonuniform in space, thus making it difficult to combine frames from multiple sweeps. Therefore, it was decided to link the ultrasound frame rate to the location of the motorized stage, triggering a series of angled plane-wave transmissions every time the stage had moved a specified distance as shown in Fig. 2, after which the ultrasound system waits for the next
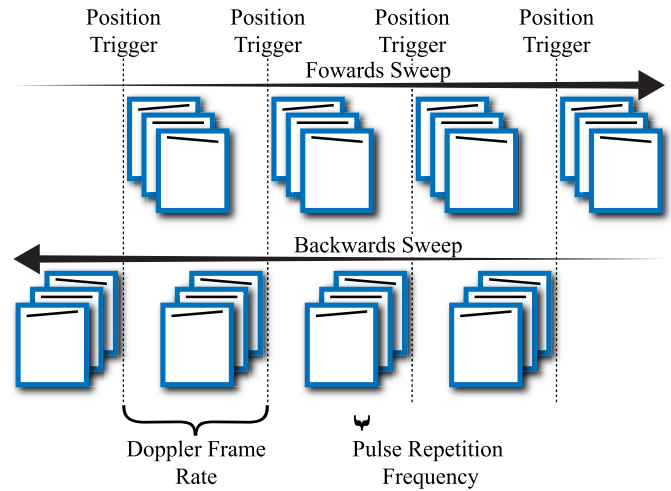

Fig. 2. Overview of swept-3-D ultrasound acquisition. While the motorized stage is continuously translating over the region of interest, a position trigger is sent to the acquisition system every time it has moved a specified distance. When the ultrasound acquisition system receives a trigger, a series of angled plane-wave transmission, are performed in quick succession.

trigger signal (referred to as the Doppler frame rate, not to be confused with the PDI frame rate, where an ensemble of Doppler frames are averaged to create a PDI). With this method, the exact location of every frame is known and can be used to combine frames acquired at the same location during multiple sweeps.

To ensure the beamformed frame was acquired as close to the position trigger as possible, the number of angled plane-wave transmissions N_a should ideally be kept as low as feasible, as due to the continuously moving nature of the swept recordings, increasing the number of angled transmissions decreases the spatial coherence of successive frames. The number of angles was set to $N_a = 8$ between ±9°, chosen based on the diminishing return in contrast for higher N_a in ultrafast ultrasound imaging shown by Bercoff et al. [20]. Another metric that influences the coherence of successive frames is the PRF, which is ideally taken as high as possible. During testing with a waveform generator, the system was able to reliably perform using a PRF of 32 kHz without heating the transducer elements significantly, and without causing issues with real-time data transfers and processing. The PRF was, therefore, set to 32 kHz between the angled plane-wave transmissions, resulting in a maximum frame rate of 32 kHz/8 angles = 4 kHz.

Due to the varying speed of the motorized stage during the sinusoidal trajectory, and the fact that the trigger distance is set to be constant over a sweep, the maximum Doppler frame rate of 4 kHz can only be obtained when the stage is moving at its maximum speed. Some example trajectories for various sine periods are shown in Table I. First, the maximum speed is calculated for an example craniotomy of 6 mm by $v_{\max} = 2\pi|\text{Amplitude}|/\text{Period}$. The minimum trigger distance is then found for a maximum Doppler frame rate of 4 kHz, this value can be programed into the motorized stage, to trigger an acquisition every time this distance is passed. If the trigger

TABLE I
RELATIONSHIP BETWEEN SINE PERIOD AND NUMBER OF
ACQUIRED FRAMES PER VOLUME

Sine Period [s] (2 sweeps)	Maximum Sine Speed [mm/s]	Min Trigger Distance [μm]	Max Frames per Volume
5	3.77	1.57	3819
4	4.71	1.96	3055
3	6.28	2.61	2291
2	9.42	3.93	1527
1	18.85	7.85	763

distance is chosen to be smaller than this value, the ultrasound acquisition system will not perform reliably causing some triggers to be missed by the acquisition system. This minimum trigger distance then results in a maximum number of frames able to be obtained for each sweep or 3-D volume.

The table shows that using a relatively high sine period, for example, 5 s (which implies a full volume is created every 2.5 s), a maximum of 3819 frames can be acquired over the 6 mm. For a period of 2 s, which equates to 1 volume per second, only 1527 frames can be acquired over the same distance, meaning this tradeoff needs to be seriously considered depending on the duration of the functional stimulus.

C. System Hardware

To achieve 3-D fUS of the mouse brain in a swept manner, a 128-element high-frequency linear array transducer (L22-14v) was attached to a high-precision motorized linear stage (Zaber X-LDA025A) using a custom 3-D printed, lightweight encasing, and coupled to a Verasonics acquisition system (Vantage 256 High Frequency), as shown in more detail in Part I of this article. While it is not inherently necessary to remove the default housing of the transducer to perform swept-3-D fUS, we felt that the reliability of the overall system when sweeping at high speeds was improved by doing so.

The stimulation paradigms for fUS were controlled using an Arduino MKR Zero board due to its built-in real-time clock (RTC). Other microcontroller boards without an RTC, such as the Arduino UNO and Adafruit Metro M4 Grand Central experienced a significant clock drift during functional recordings, causing the functional paradigm and ultrasound recording to run out of sync. At the start of a functional recording, the data acquisition PC sends a message to the microcontroller containing the ON and OFF times of the functional paradigm through a universal serial bus connection, after which the microcontroller would run through the functional paradigm as requested in parallel to the ultrasound acquisition.

For a visual stimulation paradigm, a photograph of the ultrasound setup can be seen in Fig. 3. The visual stimulation red-green-blue LEDs (WorldSemi WS2812B Rev A) were connected to the pulsewidth modulation (PWM) ports of the Arduino through a ~1-m cable. A round cylinder was placed over the LEDs to funnel the light in a more focused direction as during recordings it was found that the light reflections caused significant functional response in the PDI signal. The LED was programed to always emit a white light during the stimulation ON periods, while the LED intensity and flickering frequencies were varied during experimentation.
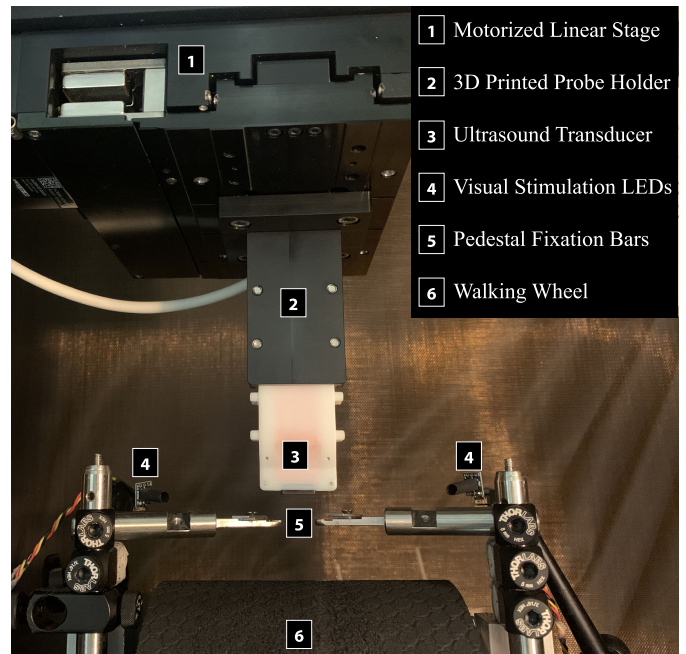

Fig. 3. Photograph of the visual stimulation experimental setup used in this article, with labels for each of the main components.

Labels: 1 Motorized Linear Stage; 2 3D Printed Probe Holder; 3 Ultrasound Transducer; 4 Visual Stimulation LEDs; 5 Pedestal Fixation Bars; 6 Walking Wheel

D. In Vivo Functional Ultrasound

All experiments were performed on adult mice (12–14 weeks of age) with a C57BL6/J background. The mice were healthy and specific pathogen-free (SPF). The animals were group-housed in a vivarium with controlled temperature and humidity, and a 12/12 h light/dark cycle with access to food and water ad libitum. After surgery, the mice were single-housed. Ethical approval was granted before the start of the experiments from the national authority (Centrale Commissie Dierproeven, The Hague, The Netherlands; license no. AVD1010020197846) as required by Dutch law, and all experiments were performed according to institutional, national, and European Union guidelines and legislation.

Surgery: To ensure head fixation during experiments, mice underwent a pedestal surgery. The mice were anesthetized using an isoflurane/oxygen mixture. The induction of anesthesia involved using 5% isoflurane, followed by a maintenance level of 1.5%–2%. A constant body temperature of 37 °C was maintained throughout the surgery. To protect the eyes from drying out an eye lubricant (Duratears) was applied. After fixation of the animal in a stereotaxic device (Stoelting), a sagittal scalp incision was made (2–3 cm). The then exposed periosteum was carefully removed, and the pedestal [Fig. 4(b)] was placed on the skull using Optibond primer and adhesive (Kerr, Bioggio, Switzerland) as well as Charisma (Heraeus Kulzer, Armonk, NY, USA) for securing the pedestal. Next, a craniotomy (Bregma +2 mm to Bregma −4 mm in length, and 7-mm width) was made, within the full size of the applied pedestal. The cranial window was then covered with a transparent TPX film (CS Hyde Company, IL, USA). The surgical procedure typically took 60–90 min. After surgery, mice were given 3–5 days to recover.

In Part I of this article, swept-3-D recordings were obtained on anesthetized mice, as the goal was to obtain the best
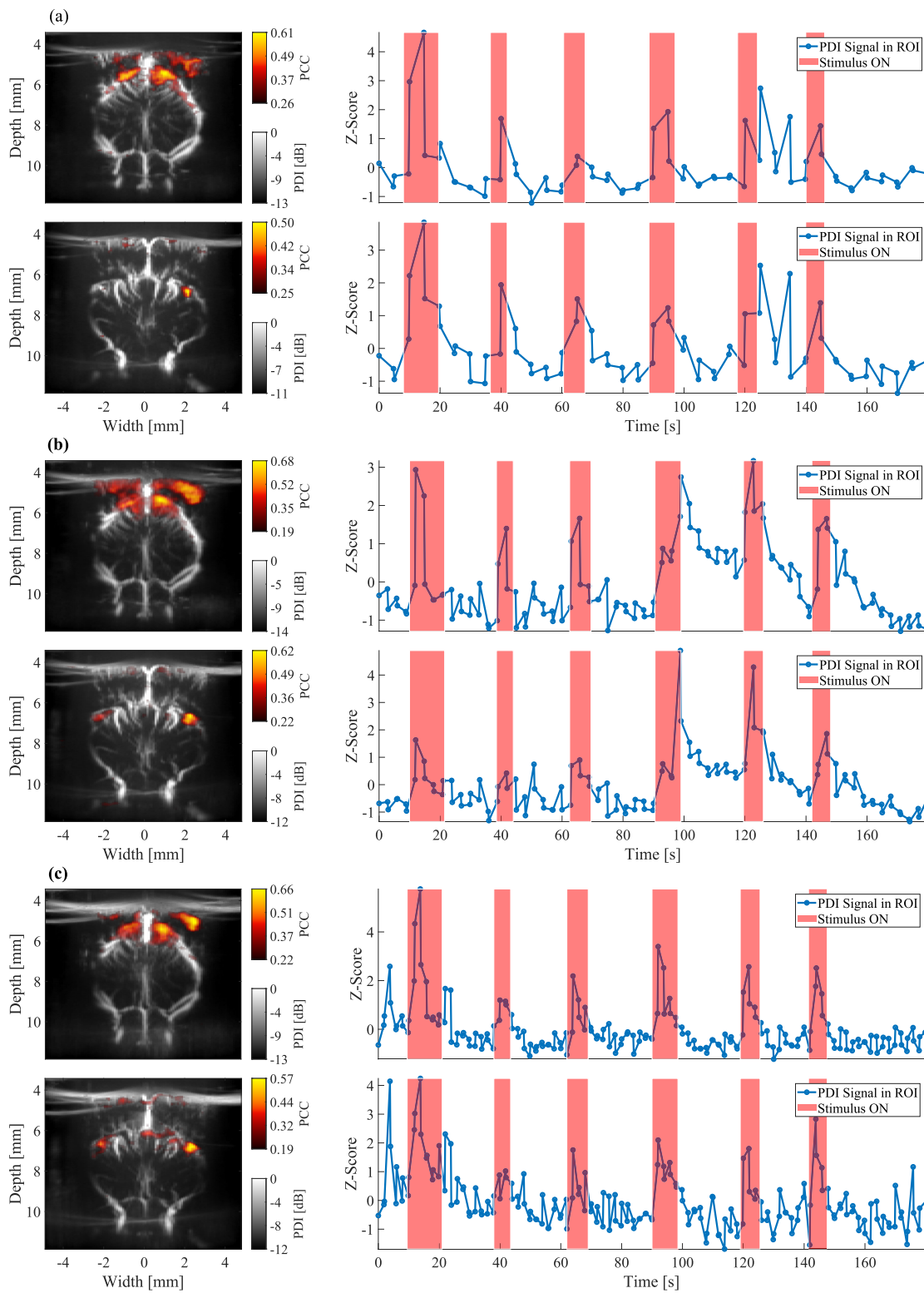
Fig. 4. Swept 3-D fUS using varying translation speeds. For volume rates of 2.5, 1.5, and 1 s per volume in (a)–(c), respectively, two PDIs are reconstructed at functional regions, with the PCC overlaid in red. On the right, the temporal component of the functionally significant pixels is shown with the applied stimulation signal. Due to the slower translation speeds in (a), a better quality PDI can be reconstructed, but the time course shows few samples when compared to the faster translation speeds of (b) and (c), due to the lower amount of sweeps completed in the same amount of time.

vascular images. Anesthetized recordings have some advantages over recordings where the rodent is awake and freely moving such as: 1) the possibility for a larger craniotomy

allowing for imaging of the lateral sections of the brain, which are often covered by the edges of the craniotomy; 2) during an anesthetized recording the brain can be exposed
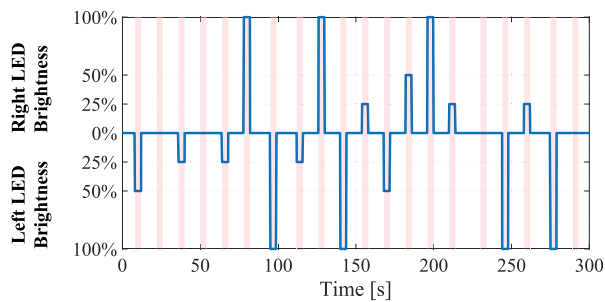
Fig. 5. Example visual stimulation paradigm using two LEDs while varying the LED brightness during the ON periods (highlighted by the red backgrounds) between 0% (OFF), 25%, 50%, and 100% of the maximum brightness value.

allowing for better acoustic coupling and therefore better SNR when compared to awake rodent recordings which require an acoustically attenuating window to be placed over the craniotomy to protect the brain; and 3) recordings on anesthetized rodents have significantly reduced motion artifacts due to the restriction of the rodents movement. Motion artifacts during awake recordings are significantly reduced by using a well-fixated pedestal, shown in Fig. 3(b), and stable fixation bars shown in our setup in Fig. 3(a).

The importance of awake recordings for functional imaging has been shown in multiple studies [21], [22] due to the effect of anesthetics on hemodynamics. Pisuaro et al. [12] found that HRs were significantly larger and faster in awake recordings when compared to those where anesthesia was used. Awake and freely moving rodent recordings also allow for testing of additional functional paradigms that are not possible under anesthesia, such as behavior studies.

E. Filtering and Reconstruction

For each swept-3-D sweep, a stack of beamformed frames of dimension (n_z, n_x, n_y) were obtained, where n_z and n_x are the spatial samples along the z- and x-directions, respectively, and n_y is the total number of beamformed frames in a sweep. Due to a swept-3-D sweep containing frames obtained at unique locations, with a fixed distance between them, we have ample freedom in how to combine beamformed frames as well as the spatial interval at which we create frames. For instance, if we want to create a PDI every 100 μm, we can simply create an ensemble of frames around that location of dimensions (n_z, n_x, n_e) and filter out the stationary tissue components using conventional methods such as a singular value decomposition (SVD) [23], [24], [25]. The threshold for the number of SVD components to remove was chosen manually, after which a PDI was created by averaging over the ensemble. This process is then repeated for the full sweep, creating PDIs at the set step size. The amount of frames taken for each ensemble depends on the speed of the motorized stage, as it influences the distance between the acquisition of successive beamformed frames and therefore the amount of shared content between them, as was discussed at length in Part I of this article.

III. Swept-3-D Functional Ultrasound

A. Swept-3-D fUS Validation

To validate the swept-3-D method on a functional recording, a series of simple visual stimulation experiments were performed while the motorized stage was translated over the brain at varying speeds. As mentioned in Section II-A, the speed at which the motorized stage moves back and forth over the brain influences the sampling at each location as well as the resulting quality of the PDIs. While a slow translation speed is desired for high SNR PDIs, a fast translation speed is desired for better sampling of the functional fluctuations. Nunez-Elizalde et al. [11] mentioned that the fUS signal strongly correlates with the slow, <0.3-Hz fluctuations in the local firing rate, and Bertolo et al. [7] advised that while quickly scanning the brain for fUS, a volume sampling frequency of at least 0.4 Hz was recommended, which is equal to performing one full sweep in at most 2.5 s. Bertolo et al. [7] were limited by having to start and stop the motorized stage to perform a stationary acquisition for every slice, which limited either the number of scanned slices or the volume rate.

By continuously moving over the brain, we can achieve high volume rates while still being able to reconstruct PDIs at small spatial intervals. A functional recording was performed in the setup shown in Fig. 3(a), where a 3-Hz blinking white light LED was shown on the left side of the mouse during intervals over a 180-s recording. The blinking LED was activated for a time chosen randomly between 6 and 12 s, followed by an OFF-period chosen randomly between 15 and 20 s to minimize the predictability of the stimulus for the mouse and improve functional signal decoupling from periodic physiological induced signals. The blinking frequency of 3 Hz was chosen as this was shown to elicit a strong functional response in a previous study [26] and falls in line with typical values used such as 5 Hz [8] and 4 Hz [7]. The same functional paradigm was repeated while the motorized stage was set to oscillate from the back of the TPX window to the front with three different sine periods of 5, 3, and 2 s (resulting in a volumetric volume rate of 2.5, 1.5, and 1 s per volume).

The resulting functional maps for each of the speeds are shown in Fig. 4(a)–(c), respectively. Fig. 4(a) shows two PDIs reconstructed at two different locations along the mouse brain for a sine period of 5 s (creating a volume every 2.5 s). For every pixel of each PDI, the time series is correlated with the known applied stimulation pattern, and the Pearson correlation coefficient (PCC) is overlaid on the PDIs.

For each of the overlaid functional maps shown in this article, the lower threshold of the image was set to the activation that was considered significant, which corresponded to a pixel value greater than 2σ, where σ is the standard deviation of all the functional pixel values of the bottom 30% of the functional image (containing a combination of nonfunctional pixels inside and outside of the brain), inspired by previously shown methods [1], [26], [27].

To display the temporal component of the functional signal, the sum is taken over the temporal signals of each functionally significant pixel (pixel value $> 2\sigma$), each weighted by
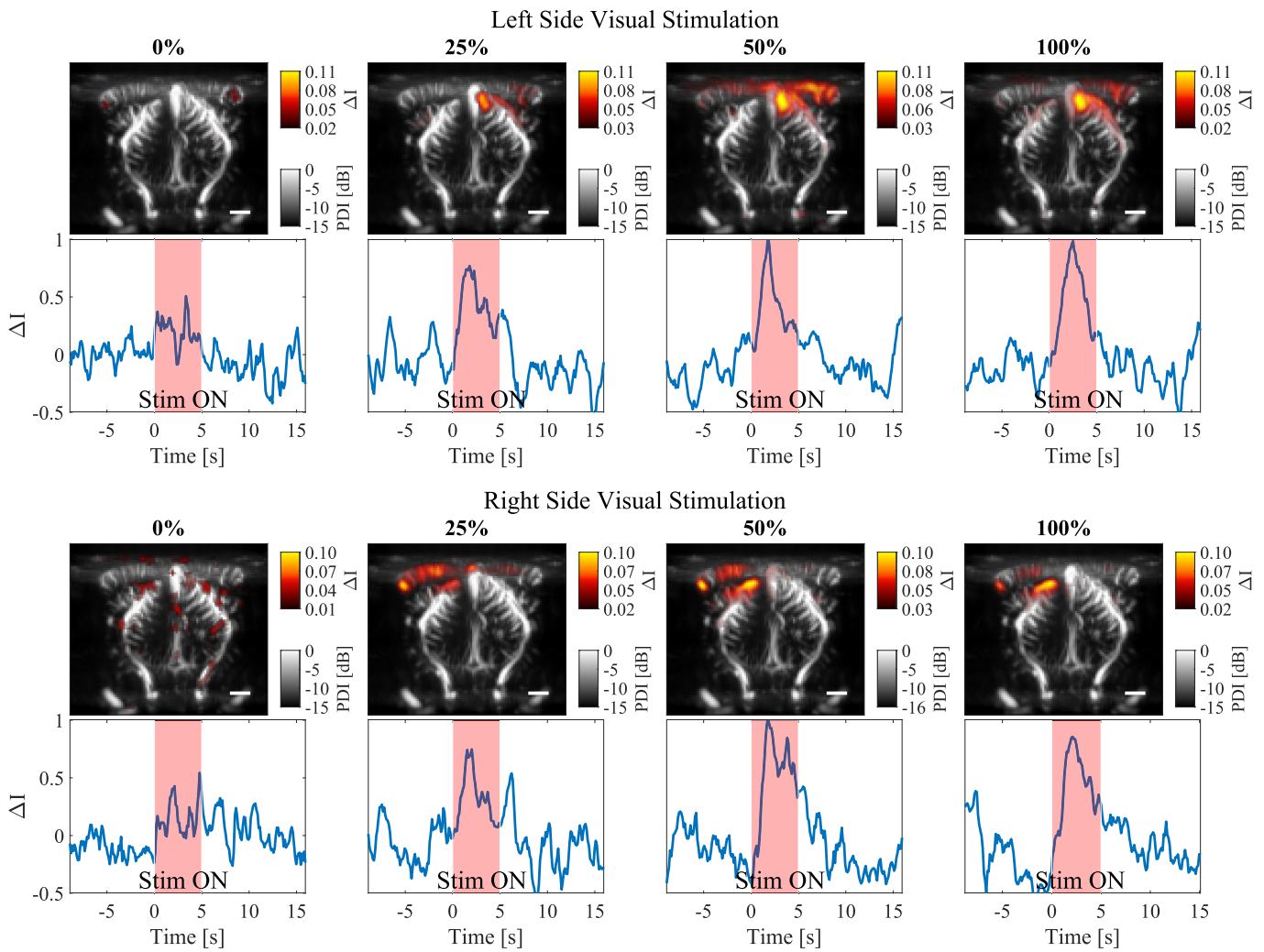
Fig. 6.   Stationary visual stimulation fUS at a single imaging location while varying the LED brightness between 0% (OFF), 25%, 50%, and 100% of the maximum brightness value (columns) for an LED placed on the left side (top) and the right side (bottom). For each occurrence of each stimulation, the ratio is calculated between the signal during the ON-period and the OFF-period for each pixel, and the ΔI is calculated by averaging over each reoccurring stimulation. This ΔI image is overlaid on the gray-scale PDI in red. The displayed temporal signal is calculated by weighting all functionally significant pixels as described in Section III-A. The resulting signal is then z-scored and also averaged over the repeated stimulations (~7 repeats) to show how the signal changes in response to the applied stimulation. The white bar overlaid on the PDI indicates a distance of 1 mm.

multiplying it by the corresponding functional pixel value. The resulting array is then divided by the sum of all functionally significant pixels.

The calculated temporal signal for the significant functional pixels, together with the stimulus signal are shown on the right for each of the two locations. Here, we can see that the PDI signal follows the applied stimulation paradigm, even though at times only two samples are available during a stimulation-ON period. For the reconstruction of these PDIs, the stationary components were mostly filtered out resulting in good-quality PDIs. Fig. 4(b) and (c) shows the same for sine periods of 3 s (volume rate of 1.5 s per volume) and 2 s (volume rate of 1 s per volume). While the temporal sampling shown in Fig. 4(c) is the highest, the quality of the PDIs is significantly deteriorated causing a lower functional sensitivity.

B. Functional Ultrasound

1) Visual Stimulation Paradigm: While the stimulation paradigm described in Section III-A used a single LED shown

on the left side, a new and more complex paradigm was created using two LEDs placed in front of the mouse on the left and right side, at about 10 cm distance and 45°. The initial experiment also only used LEDs at 100% brightness, so in this new paradigm, we decided to vary the brightness for each ON period. A third LED was added at a distance of 30 cm directly in front of the mouse, emitting a constant, low-brightness white light to suppress effects from light reflections in the setup.

A blinking LED stimulation paradigm was created using MATLAB. The stimulation ON duration was set to 5 s for every ON period, which allows us to split our functional signal into separate epochs for the left and right LED as well as individual LED brightness levels so that we can investigate each paradigm separately. The interstimulus interval (ISI) that denotes the time between the end of the last ON-period and the start of the next ON-period was picked randomly to be between 10 and 16 s for every interval. A weighting was applied for a higher chance of having lower ISIs to increase
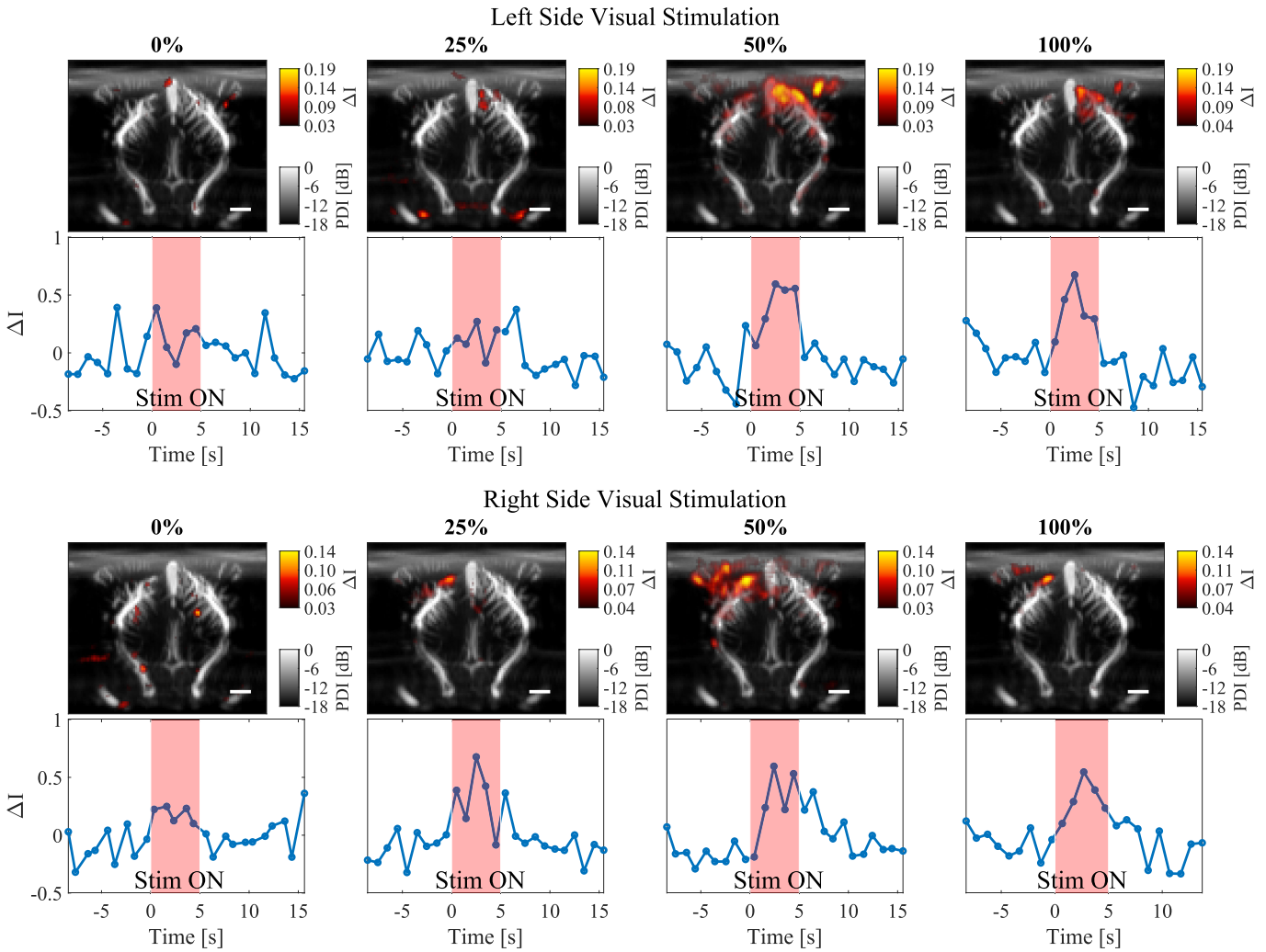
Fig. 7. Swept-3-D visual stimulation fUS, where only the PDI is shown for the slice reconstructed closest to the stationary recording shown in Fig. 6. The exact same processing was applied as in the previous stationary example, showing that as the LED brightness was increased, the response increased contralaterally for both the left and right LED stimulation, similar to what was shown in the stationary example. The number of samples obtained during each stimulation epoch is significantly reduced using the swept-3-D method when compared to the stationary recording. The white bar overlaid on the PDI indicates a distance of 1 mm.

the number of repetitions possible in the recording. During the ON-periods, one of the two LEDs (either right or left) was set to blink at 3 Hz, where the brightness of the LED was selected randomly between four values: 0% (OFF), 25%, 50%, and 100% of the maximum brightness value. The total recording duration was set to 20 min, to allow for enough repeats of each of the different LED brightness. An example of the first 5 min of a stimulation paradigm is shown in Fig. 5 showing for the left and right LEDs which brightness would be presented at what time.

2) Swept-3-D Visual Stimulation Results: For every mouse ($n = 5$), a functional swept-3-D recording of 20 min was performed followed by a single stationary recording at a location toward the posterior of the craniotomy, where the superior colliculus (SC) and VISp were thought to be present. For each, the same visual functional paradigm was presented during the recording and the data was stored for postprocessing.

For the swept-3-D recording, the transducer was set to move back and forth over the mouse brain from just over craniotomy

edges at a sine period of 3 s (creating a volume every 1.5 s). The ultrasound acquisition parameters were kept as described in Section II, using an ensemble of 200 beamformed frames to form a PDI.

For recordings using this updated stimulation paradigm, it was less intuitive to use the PCC to calculate functional activation, as a single recording contains multiple different stimuli presented to the mouse in a randomized order. Therefore, the PDI signal over time was split into short time series, or epochs, for each of the different LED locations and intensities, allowing for approximately nine repeats of every combination. Every epoch consisted of time series starting from 8 s before the onset of the visual stimulation, till 15 s after the onset. The ratio between the ON/ and OFF periods was calculated by averaging the PDI signal during the ON period for every pixel (from 0 to 5 s), subtracting the baseline value (average PDI value between -8 and 0 s, and 6 and 15 s) and dividing by the baseline value, referred to as the delta intensity or ΔI. The $t - 8$ was chosen as the start
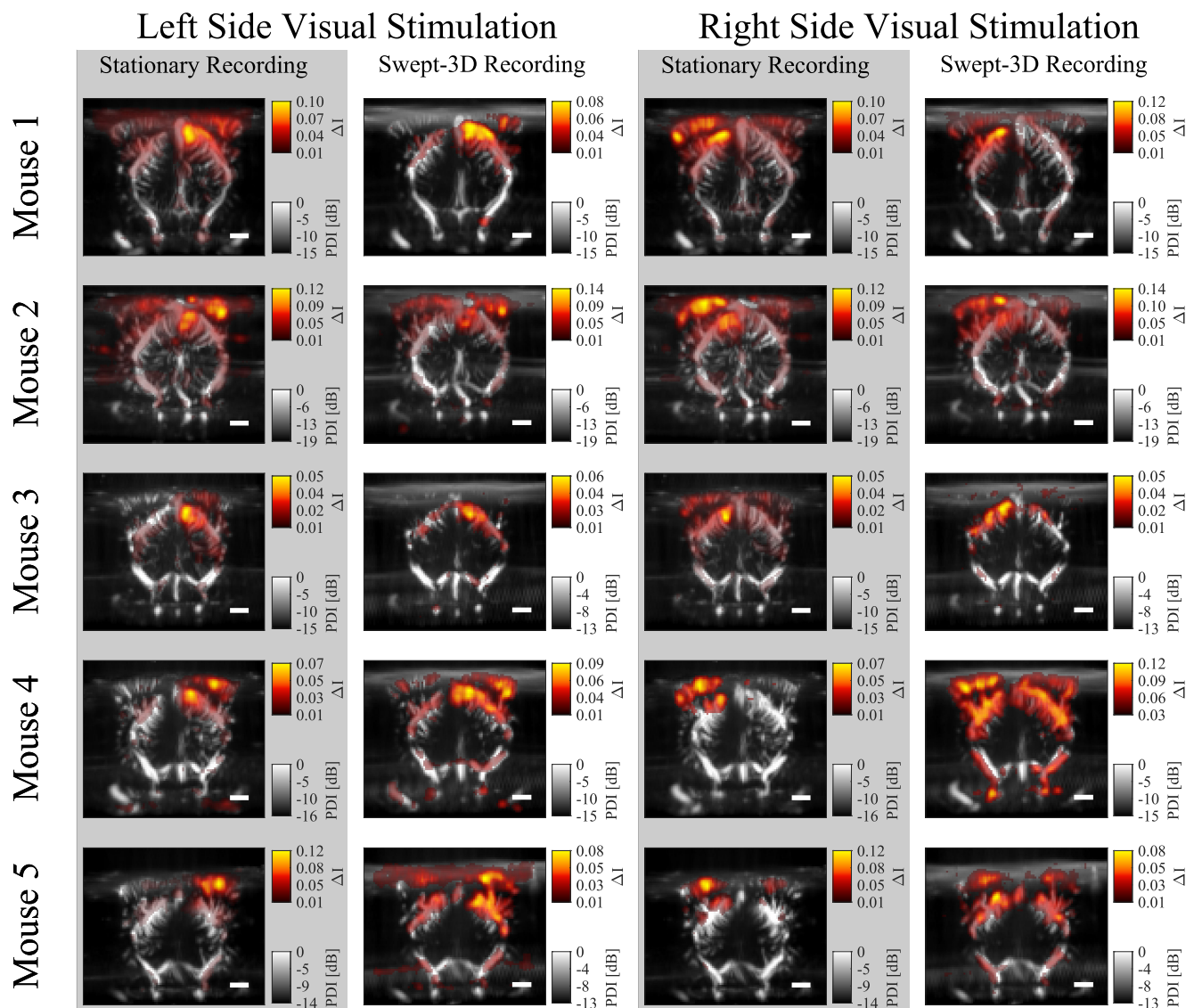
Fig. 8. Comparing functional activity between stationary and swept-3-D functional recordings for $n = 5$ mice. For each swept-3-D recording, a PDI was reconstructed at the closest location to the stationary recording. The LED brightness levels of 25%, 50%, and 100% were combined for both the left and right LED, and the ΔI image was created for both the stationary and swept-3-D recordings and overlaid on the corresponding PDI. The white bar in the bottom right indicates a 1-mm distance.

of the baseline as there were at least 10 s between the end of the last stimulation-ON period and the current one. The same applies for the baseline after the current 5 s ON period, where $t + 6$ was chosen with a safety margin for the HRF to return to baseline, and $t + 15$ is the maximum time before the next stimulation-on could appear. Every ΔI image of dimensions (n_z, n_x) was grouped with the ~9 intensity maps created during the same stimulus intensity and location, and the median absolute deviation (MAD) was calculated between the stack of ΔI images, and two images with the highest MAD were removed, after which the average ΔI image was created by averaging over the remaining ~7 frames. The ΔI image was then overlaid on the gray-scale PDI reconstructed for that location.

The results for the stationary recording are shown in Fig. 6 for the left and right side visual stimulation. For each column, the LED brightness is shown as a percentage of the maximum

value on the top. For visualization, the z-score is calculated for the functional temporal signal of every epoch, calculated using the same method as described for the PCC in Section III-A. These weighted temporal signals are then averaged to show how the signal changes when the stimulus is presented to the mouse and is displayed under every corresponding PDI. Functional activation appears contralaterally in both the VISp and SC, for both the left and right LEDs. We can see that when the brightness was set to 0%, used as a control, no response was present during the onset of the visual stimulation. As the brightness was increased the response also increased, and most likely saturated between the 50% and 100% of the maximum LED brightness level.

The results for a swept-3-D fUS recording, using the same visual stimulation paradigm, are shown in Fig. 7. As expected, due to the volume rate of 1.5 s per volume, a lot less samples are acquired for each location when compared to the stationary
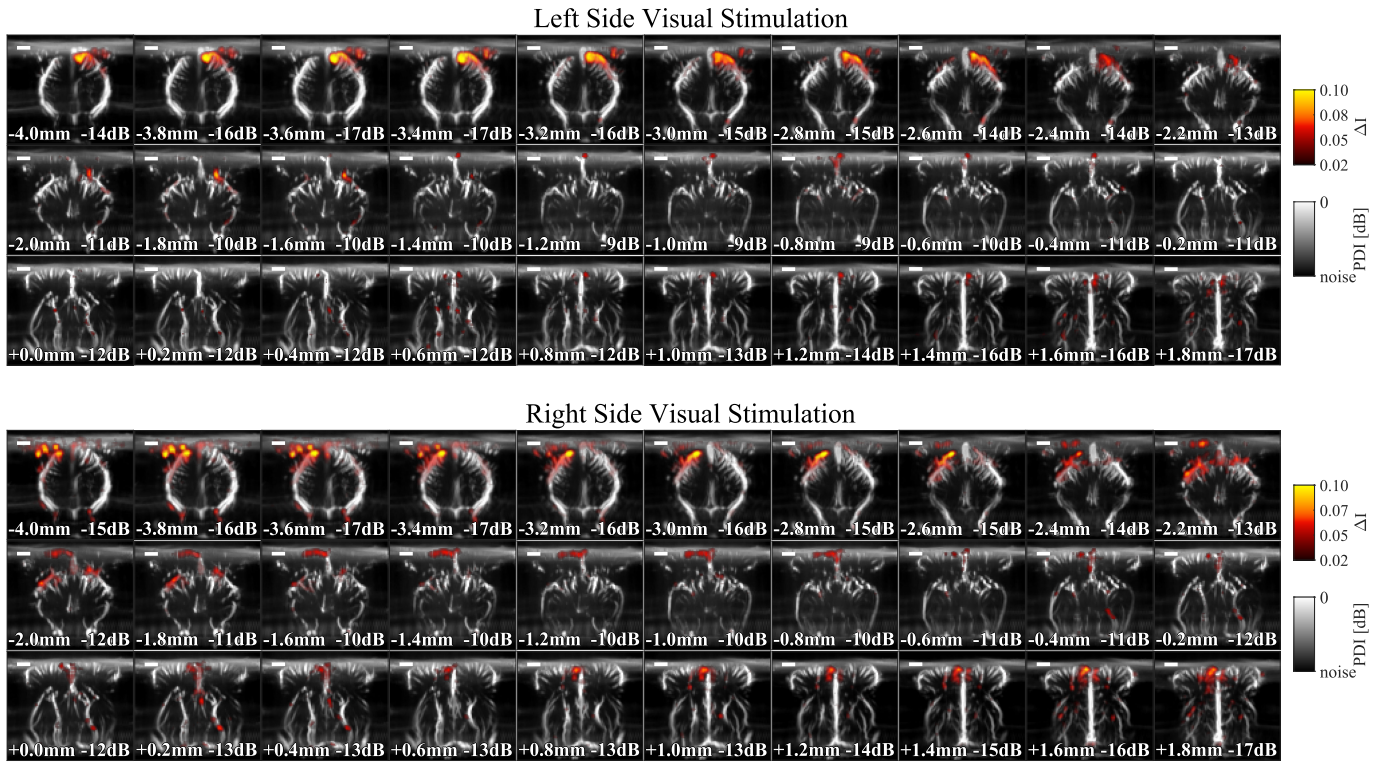
Fig. 9. Volumetric swept-3-D fUS using a visual stimulation paradigm. The PDIs were reconstructed every 200 μm starting from the most caudal slice (top left) to the most rostral slice (bottom right), and the ΔI was calculated by combining the LED brightness levels of 25%, 50%, and 100%. The white bar in the top left indicates a 1 mm distance.

recording shown in Fig. 6. However, the VISp and SC still appear as functional regions in the ΔI overlay, and the same trend of increasing ΔI for increasing LED brightness can be found for both the left and right LED.

This functional paradigm was repeated for $n = 5$ mice, where a stationary recording was performed right after the swept-3-D functional recording. A PDI was reconstructed for the swept-3-D method at the location closest to the stationary recording, and the same processing as discussed in Section III-B2 was performed on both the stationary and swept-3-D data to create a ΔI overlay, where the brightness levels of 25%, 50%, and 100% were combined to increase functional sensitivity. The results are shown in Fig. 8 for both the left and right side visual stimulations.

The advantage of the swept-3-D technique is that, unlike a single stationary recording, these functional activity maps can be created for the full brain using this single recording. For the recording shown in Fig. 7, a PDI is reconstructed every 200 μm starting from the most posterior slice toward the most anterior slice and shown in Fig. 9. The step size of 200 μm was chosen purely for convenience to display the results, as the distance between successive beamformed frames is much lower. For each reconstructed PDI, the same processing was performed as in the previous figure, except the ΔI images from LED brightness levels of 25%, 50%, and 100% were combined to increase the functional sensitivity, resulting in a single overlaid ΔI image for every PDI. This gives us volumetric fUS using a continuously moving linear stage, while only performing a single functional recording.

IV. DISCUSSION AND CONCLUSION

The goal of this article was to perform volumetric fUS using a continuously moving 1-D-array ultrasound transducer. This was achieved by sweeping back and forth over the brain at a high speed so that every location in our 3-D volume was sampled at a high enough rate to accurately sample the HR to our visual stimulation paradigm. We initially demonstrated the viability of swept-3-D fUS by using a simple visual stimulation paradigm and varying the trajectory speed (Fig. 4). We showed that while sweeping over the brain slowly is beneficial for the PDI SNR and clutter filtering properties, higher translation speeds allow for better sampling of the HR in the Doppler signal so it is important to find a good middle ground. A larger study was conducted on $n = 5$ mice using a more complex visual stimulation paradigm, where an LED was placed on the left and right sides of the mouse, and the brightness was altered between 0% (OFF), 25%, 50%, and 100% of the maximum brightness value of the LED (Fig. 5). Results from our swept-3-D method were compared to stationary recordings in Figs. 6 and 7, where both methods showed higher functional responses as the brightness level was increased. For Fig. 8, the Doppler signal of brightness values of 25%, 50%, and 100% were combined to increase functional sensitivity, after which our swept-3-D method was compared to a stationary recording for $n = 5$ mice. While the results of our method appear comparable to the stationary recording for the PDI reconstructed closest to the location of the stationary recording, our swept-3-D method can reconstruct volumetric 3-D fUS using a single functional recording (Fig. 9).

The goal of using the visual stimulation paradigm shown in Section III-B1 was to be able to show the influence of LED brightness on functional activation. The first issue we encountered was that the light of the LEDs caused reflections in the enclosure, causing activation in the ipsilateral side of the brain. This effect was minimized by adding tubes to the LED that kept the light more focused. In addition, a third LED was added directly in front of the mouse with a constant, but low brightness level to apply a constant low-level stimulation, and therefore decrease the significance of the reflections.

Previous studies using fUS typically relied on sensory stimuli lasting for tens of seconds [7], [9], [26]. Here, we wanted to know whether our swept-3-D technique can record neurovascular signals associated with much shorter stimuli, for which reason we present visual stimuli for 5 s. In these periods, we observed—in both the stationary and swept-3-D functional recordings—a fast increase in the PD signal, followed by a rapid decay. Such kinetics are in line with the fast adaptation observed in electrophysiological recordings made in the SC during a prolonged stationary visual stimulus [28]. We conclude, therefore, that swept-3-D recordings faithfully represent the neural signal with a relatively high temporal resolution.

Some of our swept-3-D recordings appear to have significant motion artifacts, causing a significant portion of the image to be highly correlated with the stimulus, such as during the right side visual stimulation of mouse 4 in Fig. 8, which could also potentially be solved by increasing the stimulation ON and OFF periods. As shown in Fig. 1, the brain regions related to the visual stimulation paradigm are close to the caudal edge of the sweeping trajectory, and even extend beyond the limits of a common craniotomy. The sampling of our swept-3-D method is more irregular toward the trajectory boundaries, potentially negatively impacting our functional sensitivity for the visual areas. Extending the craniotomy further caudally can lead to complications during surgery due to the large superficial sinus vein, and therefore was not performed for this study.

In this article, we show 3-D fUS on the mouse brain, as due to the small organ size, it is well suited for performing fast sweeps over it. Translating the linear sweep geometry to the human brain will likely become impractical using the current implementation due to the increased surface and curvature in a clinical setting, which will require additional solutions to maintain proper acoustic coupling along the linear translation trajectory. In addition, clinical transducers are typically larger and heavier than those used on the mouse brain, and the aperture does not fully cover the lateral expanse of the brain as is often the case with the mouse brain. A more suited direction could be the use of fanning beams such as provided by Wobbler probes [29], or recent work by Dong et al. [30] where fast tilting acoustic reflectors are used to scan the area of interest. There are clear parallels between swept-3-D fUS and fMRI, and therefore it may be beneficial to take inspiration from advances in signal-processing techniques from fMRI as that field is more established.

In conclusion, for Part II of this article, we focus on creating PDIs with the highest functional sensitivity while scanning the brain in a swept fashion. We achieved this by translating the ultrasound transducer at a speed high enough to accurately sample the variations in Doppler signal due to an applied visual stimulation for every location along the motorized stage's trajectory, while moving slow enough to allow for good clutter filtering and averaging, and therefore good quality PDIs. Swept-3-D fUS provides us with a method to perform volumetric fUS imaging of a mouse brain in a cheap and efficient manner.

REFERENCES

[1] E. Macé, G. Montaldo, I. Cohen, M. Baulac, M. Fink, and M. Tanter, "Functional ultrasound imaging of the brain," *Nature Methods*, vol. 8, no. 8, pp. 662–664, 2011.

[2] G. Grohs-Metz, R. Smausz, J. Gigg, T. Boeckers, and B. Hengerer, "Functional ultrasound imaging of recent and remote memory recall in the associative fear neural network in mice," *Behav. Brain Res.*, vol. 428, Jun. 2022, Art. no. 113862.

[3] M. Nouhoum et al., "A functional ultrasound brain GPS for automatic vascular-based neuronavigation," *Sci. Rep.*, vol. 11, no. 1, p. 15197, 2021.

[4] C. Demené et al., "4D microvascular imaging based on ultrafast Doppler tomography," *NeuroImage*, vol. 127, pp. 472–483, Feb. 2016.

[5] É. Macé et al., "Whole-brain functional ultrasound imaging reveals brain modules for visuomotor integration," *Neuron*, vol. 100, no. 5, pp. 1241.e7–1251.e7, Dec. 2018.

[6] R. Rau et al., "3D functional ultrasound imaging of pigeons," *NeuroImage*, vol. 183, pp. 469–477, Dec. 2018.

[7] A. Bertolo et al., "Whole-brain 3D activation and functional connectivity mapping in mice using transcranial functional ultrasound imaging," *J. Visualized Exp.*, no. 168, p. e62267, Feb. 2021.

[8] C. Brunner et al., "A platform for brain-wide volumetric functional ultrasound imaging and analysis of circuit dynamics in awake mice," *Neuron*, vol. 108, no. 5, pp. 861.e7–875.e7, Dec. 2020.

[9] C. Rabut et al., "4D functional ultrasound imaging of whole-brain activity in rodents," *Nature Methods*, vol. 16, no. 10, pp. 994–997, Oct. 2019.

[10] J. Sauvage et al., "4D functional imaging of the rat brain using a large aperture row-column array," *IEEE Trans. Med. Imag.*, vol. 39, no. 6, pp. 1884–1893, Jun. 2020.

[11] A. O. Nunez-Elizalde et al., "Neural correlates of blood flow measured by ultrasound," *Neuron*, vol. 110, no. 10, pp. 1631.e4–1640.e4, May 2022.

[12] M. A. Pisauro, N. T. Dhruv, M. Carandini, and A. Benucci, "Fast hemodynamic responses in the visual cortex of the awake mouse," *J. Neurosci.*, vol. 33, no. 46, pp. 18343–18351, Nov. 2013.

[13] E. S. Lein et al., "Genome-wide atlas of gene expression in the adult mouse brain," *Nature*, vol. 445, no. 7124, pp. 168–176, 2007.

[14] R. Bakker, P. Tiesinga, and R. Kötter, "The scalable brain atlas: Instant web-based access to public brain atlases and related content," *Neuroinformatics*, vol. 13, no. 3, pp. 353–366, Jul. 2015.

[15] A.-K. Aydin et al., "Transfer functions linking neural calcium to single voxel functional ultrasound signal," *Nature Commun.*, vol. 11, no. 1, p. 2954, Jun. 2020.

[16] A. Erol et al., "Deconvolution of the functional ultrasound response in the mouse visual pathway using block-term decomposition," *Neuroinformatics*, vol. 21, no. 2, pp. 247–265, Apr. 2023.

[17] R. T. Constable, "Challenges in fMRI and its limitations," *Funct. Neuroradiol., Princ. Clin. Appl.*, pp. 497–510, May 2023.

[18] S. M. Smith, "Overview of fMRI analysis," *Brit. J. Radiol.*, vol. 77, no. 2, pp. S167–S175, Dec. 2004.

[19] E. Mace, G. Montaldo, B.-F. Osmanski, I. Cohen, M. Fink, and M. Tanter, "Functional ultrasound imaging of the brain: Theory and basic principles," *IEEE Trans. Ultrason., Ferroelectr., Freq. Control*, vol. 60, no. 3, pp. 492–506, Mar. 2013.

[20] J. Bercoff et al., "Ultrafast compound Doppler imaging: Providing full blood flow characterization," *IEEE Trans. Ultrason., Ferroelectr., Freq. Control*, vol. 58, no. 1, pp. 134–147, Jan. 2011.

[21] R. R. Peeters, I. Tindemans, E. De Schutter, and A. Van der Linden, "Comparing BOLD fMRI signal changes in the awake and anesthetized rat during electrical forepaw stimulation," *Magn. Reson. Imag.*, vol. 19, no. 6, pp. 821–826, Jul. 2001.

[22] C. Martin, J. Martindale, J. Berwick, and J. Mayhew, "Investigating neural–hemodynamic coupling and the hemodynamic response function in the awake rat," *NeuroImage*, vol. 32, no. 1, pp. 33–48, Aug. 2006.

[23] D. E. Kruse and K. W. Ferrara, "A new high resolution color flow system using an eigendecomposition-based adaptive filter for clutter rejection," *IEEE Trans. Ultrason., Ferroelectr., Freq. Control*, vol. 49, no. 10, pp. 1384–1399, Oct. 2002.

[24] L. Lovstakken, S. Bjaerum, K. Kristoffersen, R. Haaverstad, and H. Torp, "Real-time adaptive clutter rejection filtering in color flow imaging using power method iterations," *IEEE Trans. Ultrason., Ferroelectr., Freq. Control*, vol. 53, no. 9, pp. 1597–1608, Sep. 2006.

[25] C. Demené et al., "Spatiotemporal clutter filtering of ultrafast ultrasound data highly increases Doppler and fultrasound sensitivity," *IEEE Trans. Med. Imag.*, vol. 34, no. 11, pp. 2271–2285, Nov. 2015.

[26] M. Gesnik et al., "3D functional ultrasound imaging of the cerebral visual system in rodents," *NeuroImage*, vol. 149, pp. 267–274, Apr. 2017.

[27] B. F. Osmanski et al., "Functional ultrasound imaging reveals different odor-evoked patterns of vascular activity in the main olfactory bulb and the anterior piriform cortex," *NeuroImage*, vol. 95, pp. 176–184, Jul. 2014.

[28] M. Dasilva, R. Storchi, K. E. Davis, K. L. Grieve, and R. J. Lucas, "Melanopsin supports irradiance-driven changes in maintained activity in the superior colliculus of the mouse," *Eur. J. Neurosci.*, vol. 44, no. 6, pp. 2314–2323, Sep. 2016.

[29] R. W. Prager, U. Z. Ijaz, A. Gee, and G. M. Treece, "Three-dimensional ultrasound imaging," *Proc. Inst. Mech. Eng., H, J. Eng. Med.*, vol. 224, no. 2, pp. 193–223, 2010.

[30] Z. Dong et al., "High volume rate 3-D ultrasound imaging using fast-tilting and redirecting reflectors," *IEEE Trans. Ultrason., Ferroelectr., Freq. Control*, vol. 70, no. 8, pp. 799–809, Aug. 2023.

Bastian S. Generowicz was born in The Netherlands, in 1990. He received the B.Sc. degree in electrical engineering and the M.Sc. degree (electrical engineering) in the signals and systems track from the Delft University of Technology, Delft, The Netherlands, in 2016 and 2019, respectively. He is currently pursuing the Ph.D. degree with the Department of Neuroscience, Erasmus MC, Rotterdam, The Netherlands.

His field of research focused on applying advanced signal processing techniques to the field of Doppler ultrasound imaging. At present, he is developing new techniques for 3-D functional ultrasound and 3-D Doppler imaging of the brain.

Stephanie Dijkhuizen was born in Delft, The Netherlands, in 1991. She received the B.Sc. degree in biomedical science from Hogeschool Leiden, Leiden, The Netherlands, in 2016.

She joined the Associative Learning Laboratory in 2017 and the Department of Neuroscience, CUBE, Erasmus Medical Center, Rotterdam, The Netherlands, in 2019. Her current field of research focuses mainly on associative learning using Pavlovian eyeblink conditioning.

Laurens W. J. Bosman received the M.Sc. degree (cum laude) in biology from Leiden University, Leiden, The Netherlands, in 1998, and the Ph.D. degree in neuroscience from Vrije Universiteit Amsterdam, Amsterdam, The Netherlands, in 2002.

He started to study the working of the cerebellum first as a Postdoctoral Fellow together with Arthur Konnerth (Technische Universität München) and later with Chris De Zeeuw at Erasmus MC, Rotterdam, The Netherlands. Currently, he works as an Assistant Professor at the Department of Neuroscience, Erasmus MC, studying the ability of the brain to adapt actions to sensory feedback, with a particular interest in neural circuits involving the cerebellum.

Chris I. De Zeeuw was born in Gouda, The Netherlands, in 1960. He received the M.D. and Ph.D. degrees (cum laude) from Erasmus MC, Rotterdam, The Netherlands, in 1990 and 1991, respectively.

His research has led to unprecedented insights into how the brain, in particular, the cerebellum, may control simple forms of learning like adaptation and conditioning of eye movements and eye blinks.

Dr. De Zeeuw was a Co-Founder of CUBE. Since 1998, he has been the Chair of the Department of Neuroscience, Erasmus MC, as well as a Scientific Vice-Director of the Netherlands Institute for Neuroscience, Royal Dutch Academy of Arts and Sciences (KNAW), Amsterdam, The Netherlands.

Sebastiaan (Bas) K. E. Koekkoek was born in Eindhoven, The Netherlands, in 1970. He received the B.Sc. and master's degrees in medicine from Erasmus MC, Rotterdam, The Netherlands, in 1996, and the Ph.D. degree from the Department of Neuroscience, Erasmus MC, in 2004.

He was a Postdoctoral Researcher and holds a permanent position as an Assistant Professor. He is the PI of the Associative Learning Laboratory, Department of Neuroscience, and a Co-Founder of the Center for Ultrasound Brain Imaging Erasmus MC (CUBE), Erasmus MC. Next to his purely scientific work, he has been active as a General Manager of Neurasmus B.V., Rotterdam, where he was in charge of the development and valorization of new scientific tools. More recently, he operates as a Co-Founder and CSO of BlinkLab Pty, Sydney, Australia, where he oversees scientific work, creates data analysis tools, and safeguards data quality. BlinkLab develops a smartphone-based platform for neuroscience and diagnosis of neurodevelopmental and psychiatric disorders.

Pieter Kruizinga received the Ph.D. degree from Erasmus MC, Rotterdam, The Netherlands, in 2015.

In 2018, he joined the Neuroscience Department, Erasmus MC, where he leads the imaging research with the Center for Ultrasound and Brain-Imaging Erasmus MC (CUBE). His current research focuses on computational ultrasound imaging and functional ultrasound imaging of the brain.